

Rapid Automated Antenna Alignment on Robotic Antenna Ranges

Benjamin L. Moser and Joshua A. Gordon

Communications Technology Laboratory

National Institute of Standards and Technology

Boulder, Colorado 80305

Email: benjamin.moser@nist.gov, josh.gordon@nist.gov

Abstract—We present methods to automate antenna-probe alignment on a robotic antenna range using iterative fitting methods. Pose measurements are used to characterize offsets to the robot motion frame and the end effector measurement frame with minimal additional information. The fitted offsets are then used to solve the inverse kinematics problem to align the antennas. We detail variations of the approach that use external or controller-integrated kinematic models. Experimental alignments for a 3-pair antenna measurement were performed on the Large Antenna Positioning System (LAPS) robot antenna range with this technique, resulting in $7.59\mu\text{m}$ RMS position error and $40.7\mu\text{rad}$ RMS rotation error.

I. INTRODUCTION

Antenna alignment is a critical task for antenna metrology [1]. Robotic antenna ranges have increased positioning flexibility and have been adopted in a variety of settings [2]–[5]. The additional motion capability of these platforms provides an opportunity to improve alignment accuracy and reduce the total configuration time for a measurement campaign. We present a closed-loop antenna alignment method that integrates robot inverse kinematics (IK), offset estimation, and laser tracker measurements to rapidly refine Antenna Under Test (AUT) and probe alignment to achieve high final positioning accuracy.

Antenna alignment on robotic antenna ranges is currently achieved with the Move-Measure-Correct (MMC) approach [6], [7]. The difference between measured and desired antenna positions is applied as corrections to the commanded robot pose in subsequent measurement epochs. Each pose in a scan is initialized using nominal values, which requires multiple complete corrective scans before convergence is reached. A manual variant of this technique has been used for static positioning in which corrective motion is applied via the robot controller pendant by a human operator. The Move-Measure-Offset-Correct (MMOC) instead iteratively corrects each position in sequence, applying the final corrective offset from the preceding position to the nominal transform to reduce the number of fitting epochs required at a particular pose [3]. Once generated, offset positions can be stored in “correction grids” for use during repeated scans [8]. Both MMC and MMOC require manual estimation of the offsets in the robot kinematic chain, entailing additional spatial data collection and processing for each end effector mounted to the robotic positioning system.

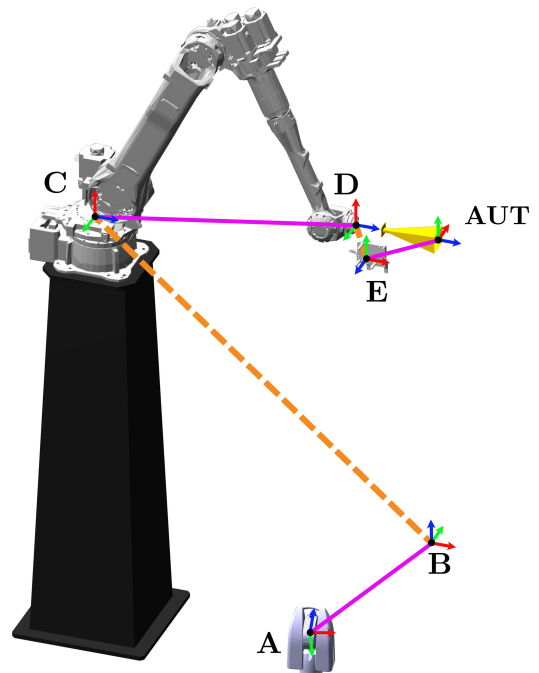


Figure 1. Illustrated frame locations for an industrial robot used for antenna metrology. A is the measurement instrument native frame, B is the laboratory frame, C is the robot base frame, D is the robot end effector frame, E is the measurement target frame, and AUT is the antenna under test frame. This frame notation is used throughout this work. Known transforms between frames are indicated with solid purple, while fitted transforms are indicated with dashed orange.

In this paper, we detail the integration of robotic kinematic modelling techniques into the antenna positioning feedback loop. In particular, we demonstrate the use of these techniques with 6 Degree-of-Freedom (DoF) laser tracker feedback to permit rapid, automated mechanical alignment of antennas without prior estimates for the robot end effector and laser tracker target offset or the laboratory frame and robot offset. The presented control loop supports both external calibrated kinematic models and native controller functionality to link the measurement and motion control of the robotic positioning system. This approach increases positioning accuracy compared to the listed robot repeatability specification and may reduce alignment times compared to existing human-in-the-loop alignment techniques.

II. METHODS

A robotic positioning system used in antenna metrology is displayed in Fig. 1 annotated with transforms \mathbf{T} describing the relative position and orientation between key locations within the measurement system. Homogeneous transformation matrices permits the evaluation of the resultant transform of the kinematic chain as

$${}^A\mathbf{T}_{AUT} = {}^A\mathbf{T}_B {}^B\mathbf{T}_C {}^C\mathbf{T}_D {}^D\mathbf{T}_E {}^E\mathbf{T}_{AUT}. \quad (1)$$

The interpretation of these transforms is as follows:

- ${}^A\mathbf{T}_B$: The offset from the measurement instrument frame to the laboratory frame.
- ${}^B\mathbf{T}_C$: The offset from the laboratory frame to the robot base frame.
- ${}^C\mathbf{T}_D$: The offset from the robot base frame to the robot end effector frame.
- ${}^D\mathbf{T}_E$: The offset from the robot end effector frame to the laser tracker target frame.
- ${}^E\mathbf{T}_{AUT}$: The offset from the laser tracker target frame to the AUT frame.

The transform between the measurement instrument and the user-defined world frame ${}^A\mathbf{T}_B$ is known directly due to the construction process, while that between the measurement frame and the AUT ${}^E\mathbf{T}_{AUT}$ can be found using laser tracker or camera-based measurement methods [9]. The transform between the robot base and end effector ${}^C\mathbf{T}_D$ is found using the nominal kinematic model native to the robot controller or an external kinematic model produced using a calibration process. There are small differences between the manufacturer and calibrated models, but both can be used with our approach.

In this configuration, the only unknown transforms are those between the world frame and the robot base ${}^B\mathbf{T}_C$ and the end effector of the robot to the measurement frame ${}^D\mathbf{T}_E$. Determining these transforms by direct measurement of physical features on the end effector and robot requires significant measurement time when using multiple antennas. Instead, we implement an optimization approach which refines local estimates of the unknown transforms to find a desired input pose for a robot inverse kinematics that minimizes the error between the desired alignment position and the current measured position. This reduces the time constraints associated with unique measurements during an alignment and permits a high degree of automation to be implemented on both standard and custom robot kinematic software. The basic algorithm for the alignment process is displayed in Alg. 1, with subfunctions discussed in the sections below.

A. Local Offset Fitting

A local estimate of the unknown transforms is needed to begin the fitting process. An estimate can be created using a series of small motions and measurements of the end effector of the robot, referred to as “registration moves” within this work. Transformation parameters are calibrated to minimize the vertically concatenated end effector error (pose error)

Algorithm 1: Alignment Algorithm

Input : (${}^A\mathbf{T}_{des}$): Desired antenna location
Output: (${}^C\mathbf{T}_D, \theta_{align}$): Aligned robot pose or joint configuration
(${}^B\mathbf{T}_E$): Resultant frame measurement

```

1 if Not Calibrated then
2   | Generate  $N$  registration poses;
3   | for  $i \in N$  do
4     |   Move to current registration pose;
5     |   Measure and store pose  $\mathbf{T}_{meas,i}$ ;
6   | end
7   | Calculate fit for  ${}^B\mathbf{T}_C, {}^D\mathbf{T}_E$  (2);
8 else
9   | Recall calibration fit for  ${}^B\mathbf{T}_C, {}^D\mathbf{T}_E$ ;
10 end
11 do
12   | Calculate target pose  ${}^C\mathbf{T}_D$  (3);
13   | if Native Controller Kinematics then
14     |   Move to  ${}^C\mathbf{T}_D$  ;
15   | else if External Kinematics then
16     |   Calculate joint configuration
17     |    $\theta_{align} = \text{robotIK}({}^C\mathbf{T}_D)$  (4);
18     |   Move to  $\theta_{align}$ ;
19   | end
20   | Measure and append pose  $\mathbf{T}_{meas}$ ;
21   | Calculate pose error  $\mathbf{E}$  and joint delta  $\Delta\theta$ ;
22   | Calculate fit for  ${}^B\mathbf{T}_C, {}^D\mathbf{T}_E$  (2);
23 while  $rms(\mathbf{E}) > e_{tol}$  &  $\Delta\theta > \Delta_{tol}$ ;
24 Return  ${}^B\mathbf{T}_E = \mathbf{T}_{meas}$ ;

```

\mathbf{E} between the desired pose \mathbf{T}_{des} and those measured. We construct the optimization problem

$$\arg \min_{{}^B\mathbf{T}_C, {}^D\mathbf{T}_E} \|\mathbf{E}({}^A\mathbf{T}_{AUT}, \mathbf{T}_{des})\|^2, \quad (2)$$

which can be solved using a vectorized transform parameterization and nonlinear least squares methods, such as point-and-quaternion offsets [10]. The fits for ${}^B\mathbf{T}_C, {}^D\mathbf{T}_E$ are locally optimal and not globally representative. Accordingly, the registration moves and initial fit generation must be performed each time the robot joint configuration substantially changes. To permit the local fitting problem to compensate for the differences between the actual and reported robot pose ${}^R\mathbf{T}_N$, the difference between the desired and actual 6 DoF pose of the robot is calculated at each step. The three newest of these measurements are used to form the pose error \mathbf{E} for the next fitting epoch. This fitting process is called on lines 7 and 21 of Alg. 1.

B. Desired Robot Pose Calculation

The fitted chamber transforms can be used to produce a desired robot pose for use with either the native kinematic model of a robot controller or an external kinematic model that passes joint information to the robot controller.

1) *Native Robot Controller Approach*: A straightforward alignment method relies on the native manufacturer inverse kinematics model to generate joint positions from an input desired transform. The controller input for the desired transform is found by mapping the collected measurement ${}^A\mathbf{T}_E$ to the controller robot transform ${}^C\mathbf{T}_D$ as

$${}^C\mathbf{T}_D = {}^B\mathbf{T}_C^{-1} {}^B\mathbf{T}_E {}^D\mathbf{T}_E^{-1}, \quad (3)$$

where ${}^B\mathbf{T}_C$, ${}^D\mathbf{T}_E$ are the homogeneous transformation matrices of the fitted offsets. The calculation of this target pose is called on line 12 of Alg. 1. The output desired transformation matrix is then converted into a controller-compatible format, such as the position and Tait-Bryan fixed XYZ Rotation angles. These representation conversions are commonly available [11]. Thorough input checking is required to prevent unexpected robot movements as changes to the required arm configuration might be required to reach a particular input transform. The application of this location interfaces with the native IK model in the controller, which calculates required robot joint positions and applies the motion before continuing in the next refinement epoch of Algorithm 1.

2) *External Kinematic Model Approach*: In cases where a kinematic model for the robot is known by calibration or manufacturer specification, the joint space solution for each IK step can be directly calculated. Unlike the prior approach, this bypasses the native IK model of the robot controller, removing a source of input precision ambiguity and permitting the use of calibrated kinematic models without requiring controller modification. A calibrated kinematic model will reduce the time required to find the solution due to the reduced pose-error at an initial pose, but may still require corrective moves.

At each transformation fit, we find a joint configuration θ to reach the desired transform ${}^C\mathbf{T}_D$ by minimizing pose-error. The inverse kinematics problem is well-documented [11], and can be expressed as the optimization problem

$$\arg \min_{\theta} \|\mathbf{E}({}^C\mathbf{T}_D, \phi)\|^2, \quad (4)$$

where θ is a vectorized list of resultant joint angles in radians and ϕ is the robot kinematic model. This minimization problem is referred to as `robotIK` on line 16 of Alg. 1. As robot joints are commonly instrumented with geared digital encoders, conversion from the output units of rad or deg from the inverse kinematics solver to pulse counts may be required.

III. EXPERIMENTAL STUDY

A. Measurement Configuration

We study antenna alignments in the context of extrapolation measurements performed on the NIST Large Antenna Positioning System (LAPS) robotic antenna range, which is composed of two 6 DoF industrial robotic manipulators and a 7m linear rail. Robots 1 and 2 have manufacturer repeatability specifications of ± 0.15 mm and ± 0.07 mm, respectively [12].

As displayed in Fig. 2, in this measurement type the linear rail determines the principle axis of motion. Accordingly, the AUT and probe must be aligned with this direction of

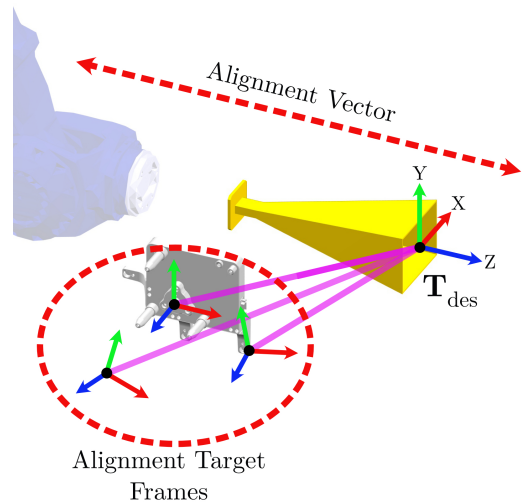


Figure 2. Detail for alignment during three-antenna extrapolation measurement. A desired AUT frame \mathbf{T}_{des} is created on the stationary robot pictured that aligns with the direction of motion of the linear rail system. Differences in antenna construction and mounting require different robot poses to achieve the same ultimate AUT alignment.

motion as well as relative to each other. In cases without a robot kinematic calibration inclusive of the rail, a best-fit line representing the axis of motion along the linear rail is constructed from a series of point measurements that are collected from a Spherically Mounted Retroreflector (SMR) mounted to Robot 1 during rail motion. A target frame is created for the stationary Robot 2, with the Z axis aligned with the linear rail axis. The rotation of the frame around this axis is arbitrary, but can be adjusted to enhance laser tracker target visibility. The corresponding target frame for the initial position of Robot 1 is then created in reference to the prior target frame. We perform alignments to satisfy a measurement approach that minimizes the number of alignments and antenna swaps required during a three-antenna extrapolation measurement, with the antenna pairs displayed in Table I. All antenna apertures are aligned to the same set of target frames within the robotic antenna range.

Table I
EXTRAPOLATION PAIR CONFIGURATION

Pair	Robot 1	Robot 2
1	Antenna A	Antenna B
2	Antenna C	Antenna B
3	Antenna C	Antenna A

The robotic arms are used for this alignment and for positioning the scan axis in the chamber, typically in an off-center configuration to minimize the impacts of secondary reflections from rail components without absorber treatment. Using the methods outlined above, we consider the alignment problem separately for each robot arm at a static rail position corresponding to the starting location of the extrapolation. By constructing target AUT and probe frames at a desired initial separation distance, the alignment procedure enforces an

accurate initial antenna separation distance with all subsequent motion performed exclusively by the linear rail.

Robot pose information is acquired using a laser tracker system (Leica Absolute Tracker AT960, Leica Geosystems)¹ with 3D SMR targets and a 6D laser tracker measurement system (TMC30-F, Leica Geosystems)¹. The laser tracker measurement accuracy is provided as $15\ \mu\text{m} + 6\ \mu\text{m m}^{-1}$ for 3D points [13]. We establish a world coordinate system that corresponds to the Robot 1 base coordinate system when positioned at the linear rail home position. The location of this coordinate system is referenced to SMR monuments mounted within the anechoic chamber for repeatable location within the measurement management software. Spatial data is acquired and stored using the Spatial Analyzer¹ software and exported for use in a LabVIEW¹ management framework.

B. Experimental Results

The automated alignment procedure was conducted for each robot three times using the same starting location and workspace. Registration moves composed of three sequential motions of the end effector by 10 deg around the principle X, Y, and Z axes were collected once per trial per robot, with the offsets retained for subsequent alignments to reduce runtime. Final alignment accuracy is reported as error for position (e_{pos}) and rotation (e_{rot}) for each of the antennas is recorded in Table II as a single RMS value for all position and rotation components with the number of fitting epochs required for convergence. The RMS of all pose-error residuals for the set of alignments of a particular antenna is also listed. The combined pose-error for all trials and robots is found as $7.59\ \mu\text{m}$ RMS position error and $40.7\ \mu\text{rad}$.

IV. DISCUSSION

The automated alignment procedure benefits robotic antenna ranges with increased positioning accuracy and reductions in manual offset characterization. The collected data demonstrates a final positioning accuracy below the manufacturer specification for both robots, which increases the maximum scan frequency while satisfying fractional wavelength criteria (e.g. $\frac{\lambda}{50}$). Due to the incorporation of offset fitting into the alignment process, the offset from the laser tracker target frame to the AUT frame is the only transform that must be externally measured. This represents a reduction in manual interaction with the alignment process compared to MMC and MMOC. Time savings resulting from this reduction vary based on manual operator proficiency, robot configuration, and algorithm exit conditions, with full quantification exceeding the scope of this work.

The presented methods provide flexibility for robot antenna ranges. Direct control of the desired end effector transforms or joint pulse information permits alignment exit conditions that

¹Certain equipment, instruments, software, or materials are identified in this paper in order to specify the experimental procedure adequately. Such identification is not intended to imply recommendation or endorsement of any product or service by NIST, nor is it intended to imply that the materials or equipment identified are necessarily the best available for the purpose.

Table II
EXPERIMENTAL ANTENNA ALIGNMENT RESULTS

Robot 1				
Antenna	Trial	$e_{\text{pos}}(\mu\text{m})$	$e_{\text{rot}}(\mu\text{rad})$	Epochs
	Combined	6.84	50.5	
A	1	6.68	45.5	5
	2	9.43	62.8	5
	3	2.64	40.3	5
	Combined	5.48	21.9	
C	1	5.14	6.36	4
	2	6.36	28.9	5
	3	4.83	23.7	4
Robot 2				
Antenna	Trial	$e_{\text{pos}}(\mu\text{m})$	$e_{\text{rot}}(\mu\text{rad})$	Epochs
	Combined	9.64	36.5	
A	1	13.2	51.7	3
	2	6.89	27.2	5
	3	7.50	24.0	3
	Combined	7.77	47.6	
B	1	8.35	53.4	6
	2	10.5	60.1	5
	3	1.44	18.7	6

can be tailored to the requirements of particular scan types and frequencies. By monitoring the change in desired joint angles, the fitting process can exit if a corrective move is too small to be registered by the encoder hardware on a particular robot. Similarly to the cached offsets in MMOC, the reuse of prior offset fits can reduce the number of registration moves and corrective epochs required for subsequent corrective moves. As implemented, the auto-alignment procedure can compensate for joint backlash effects by only approaching each move from the same, positive joint direction. A larger data set than contained in this work is needed to fully characterize the impacts of increased positioning repeatability in the context of antenna metrology uncertainty budgets.

V. CONCLUSION

We present details on an automated method of aligning antennas for scanning purposes on robotic antenna ranges. This approach integrates the robot inverse kinematics problem with offset fitting to reduce manual interactions during the antenna metrology process. We show the final accuracy of $7.59\ \mu\text{m}$ RMS position error and $40.7\ \mu\text{rad}$ RMS rotation error, which exceeds the previously reported positioning accuracy of the LAPS system. The approach allows flexible 6 DoF alignments to be performed with high accuracy and lends itself to robotic antenna platforms.

REFERENCES

- [1] C. A. Balanis, *Antenna Theory: Analysis and Design*, 4th ed. Wiley John + Sons, Apr. 2016.

-
- [2] J. A. Gordon, D. R. Novotny, M. H. Francis, *et al.*, “Millimeter-wave near-field measurements using coordinated robotics,” *IEEE Trans. Antennas Propag.*, vol. 63, no. 12, pp. 5351–5362, Dec. 2015.
- [3] P. A. Slater, J. M. Downey, M. T. Piasecki, and B. L. Schoenholz, “Portable laser guided robotic metrology system,” in *2019 Antenna Measurement Techniques Association Symposium (AMTA)*, IEEE, Oct. 2019.
- [4] R. Moch and D. Heberling, “Robot-based antenna and radar measurement system at the rwth aachen university,” in *2020 Antenna Measurement Techniques Association Symposium (AMTA)*, 2020, pp. 1–5.
- [5] D. M. Lewis, J. Bommer, G. E. Hindman, and S. F. Gregson, “Traditional to modern antenna test environments: The impact of robotics and computational electromagnetic simulation on modern antenna measurements,” in *2021 15th European Conference on Antennas and Propagation (EuCAP)*, IEEE, Mar. 2021.
- [6] D. Novotny, J. Guerrieri, and J. Gordon, “Antenna alignment and positional validation of a mmwave antenna system using 6d coordinate metrology,” en, in *2014 Proceedings of the Antenna Measurement Techniques Association*, 2014-10-13 2014.
- [7] M. S. Allman, D. Novotny, J. Gordon, A. Curtin, and S. Sandwidth, “Serial robotic arm joint characterization measurements for antenna metrology,” *AMTA 2017 Proceedings*, pp. 381–387, 2017.
- [8] J. Hatzis, P. Pelland, and G. Hindman, “Implementation of a combination planar and spherical near-field antenna measurement system using an industrial 6-axis robot,” in *AMTA 2016 Proceedings*, IEEE, Oct. 2016.
- [9] J. A. Gordon and S. S. Borenstein, “An invisible-stylus-based coordinate measurement system via scaled orthographic projection,” *Precis. Eng.*, vol. 56, pp. 211–222, Mar. 2019.
- [10] B. L. Moser, J. A. Gordon, and A. J. Petruska, “Unified parameterization and calibration of serial, parallel, and hybrid manipulators,” *Robotics*, vol. 10, no. 4, p. 124, Nov. 2021.
- [11] J. Hollerbach, W. Khalil, and M. Gautier, “Springer handbook of robotics,” in B. Siciliano and O. Khatib, Eds., *Second*. Springer, 2008, ch. Model Identification, pp. 321–344.
- [12] D. Novotny, J. Gordon, M. Allman, *et al.*, “The multi-robot large antenna positioning system for over-the-air testing at the national institute of standards and technology1,” en, in *Proceedings of the Antenna Measurement Techniques Association, Atlanta, GA, US*, Proceedings of the Antenna Measurement Techniques Association, Atlanta, GA, US, 2017-12-31 05:12:00 2017.
- [13] Hexagon Manufacturing, *Leica absolute tracker at960 data sheet*, Cedar House, 78 Portsmouth Road Cobham, Surrey KT11 1AN United Kingdom, Mar. 2022.